# Gap Junctional Coupling in Lenses from $\alpha_8$ Connexin Knockout Mice

George J. Baldo,[1] Xiaohua Gong,[2] Francisco J. Martinez-Wittinghan,[1] Nalin M. Kumar,[2] Norton B. Gilula,[2] and Richard T. Mathias[1]

[1] Department of Physiology and Biophysics, State University of New York, Stony Brook, NY 11794

[2] Department of Cell Biology, The Scripps Research Institute, La Jolla, CA 92037

ABSTRACT Lens fiber cell gap junctions contain $\alpha_3$ (Cx46) and $\alpha_8$ (Cx50) connexins. To examine the roles of the two different connexins in lens physiology, we have genetically engineered mice lacking either $\alpha_3$ or $\alpha_8$ connexin. Intracellular impedance studies of these lenses were used to measure junctional conductance and its sensitivity to intracellular pH. In Gong et al. (1998), we described results from $\alpha_3$ connexin knockout lenses. Here, we present original data from $\alpha_8$ connexin knockout lenses and a comparison with the previous results. The lens has two functionally distinct domains of fiber cell coupling. In wild-type mouse lenses, the outer shell of differentiating fibers (see Fig. 1, DF) has an average coupling conductance per area of cell–cell contact of ~1 S/cm$^2$, which falls to near zero when the cytoplasm is acidified. In the inner core of mature fibers (see Fig. 1, MF), the average coupling conductance is ~0.4 S/cm$^2$, and is insensitive to acidification of the cytoplasm. Both connexin isoforms appear to contribute about equally in the DF since the coupling conductance for either heterozygous knockout (+/−) was ~70% of normal and 30–40% of the normal for both −/− lenses. However, their contribution to the MF was different. About 50% of the normal coupling conductance was found in the MF of $\alpha_3$ +/− lenses. In contrast, the coupling of MF in the $\alpha_8$ +/− lenses was the same as normal. Moreover, no coupling was detected in the MF of $\alpha_3$ −/− lenses. Together, these results suggest that $\alpha_3$ connexin alone is responsible for coupling MF. The pH- sensitive gating of DF junctions was about the same in wild-type and $\alpha_3$ connexin −/− lenses. However, in $\alpha_8$ −/− lenses, the pure $\alpha_3$ connexin junctions did not gate closed in the response to acidification. Since $\alpha_3$ connexin contributes about half the coupling conductance in DF of wild-type lenses, and that conductance goes to zero when the cytoplasmic pH drops, it appears $\alpha_8$ connexin regulates the gating of $\alpha_3$ connexin. Both connexins are clearly important to lens physiology as lenses null for either connexin lose transparency. Gap junctions in the MF survive for the lifetime of the organism without protein turnover. It appears that $\alpha_3$ connexin provides the long-term communication in MF. Gap junctions in DF may be physiologically regulated since they are capable of gating when the cytoplasm is acidified. It appears $\alpha_8$ connexin is required for gating in DF.

KEY WORDS: pH gating • coupling conductance • $\alpha_8$ connexin Cx50 • $\alpha_3$ connexin Cx46

## INTRODUCTION

The lens is a multicellular syncytial tissue that has several structurally and functionally distinct domains. A single layer of epithelial cells covers the anterior hemisphere (see Fig. 1). At the equator, the epithelial cells begin to differentiate and elongate into fiber cells, which are laid down in shells to form the bulk of the lens mass. Thus, the oldest fiber cells are near the lens center, and the youngest are at the periphery. The fiber cells are flattened hexagons in cross section, with dimensions of ~3 × 9 μm (see Fig. 1). They extend from the anterior to posterior sutures, where they are bound together. The fiber cells pack closely together with the extracellular spaces of ~10 nm in width, thus, the volume of extracellular space is ~200 times smaller than the volume of intracellular space. The surface to volume ratio of a fiber cell is ~6,000 cm$^{-1}$, so a small mouse lens of diam 0.2 cm has ~25 cm$^2$ of fiber cell membrane, whereas the outer surface of such a lens has an area of ~0.13 cm$^2$. In the lenses of larger mammals, this disparity in areas is much larger.

The lens is the only transparent tissue that is more than a few cell layers thick. Its large size and need for transparency have posed some unique problems that have led to interesting physiological solutions, many of which appear to involve fiber cell gap junctions. Consider the problems: tissues the size of the lens are generally vascularized to enable access of metabolites to interior cells. However, blood vessels absorb and scatter light, so the lens is avascular. Thus, interior cells of the lens are a long distance from a source of metabolites. Intracellular organelles also scatter light and make most cells translucent, hence, the majority of lens cells, the mature fibers (see Fig. 1, MF), have disposed of their organelles. These cells cannot divide or make new protein, so gap junctions and other proteins must survive for the life of the organism without renewal. Finally, to focus images on the retina, the lens needs a relatively high index of refraction, which is a property of

Address correspondence to Richard T. Mathias, Department of Physiology and Biophysics, State University of New York, Stony Brook, NY 11794-8661. Fax: (631) 444-3432; E-mail: rtmathias@physiology.pnb.sunysb.edu

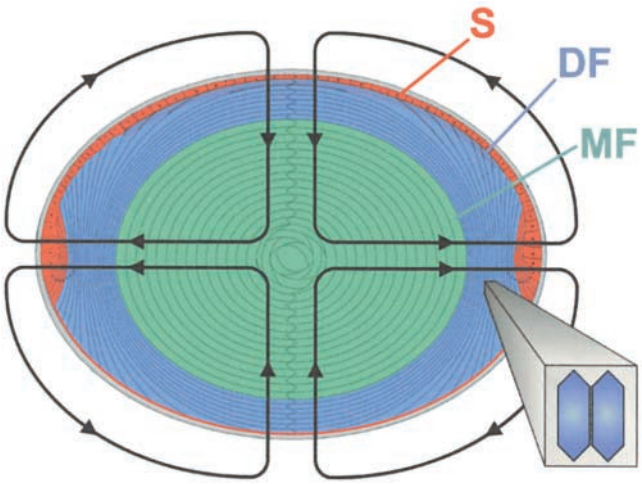


FIGURE 1. The cellular structure of the lens. Based on transport properties, the lens can be divided into three radial zones. The surface (S) includes the basal lateral membrane of the anterior epithelium and the basal membrane of differentiating fibers (DF) cells in contact with the posterior surface. These membranes have a relatively high permeability for $K^+$ and perform nearly all of the active transport in the lens. The DF and mature fibers (MF) are in communication with each other and with the surface membranes through an extensive network of gap junctions. However, the functional and structural properties of gap junctions coupling DF and MF differ, so these two domains are studied separately.

the cytoplasm of lens fiber cells. However, the extracellular spaces between fiber cells of the lens have a lower index of refraction, so their width must be less than the wavelength of visible light, otherwise they reduce transparency. This requires that lens cells precisely maintain a constant volume, since a 10% reduction in intracellular volume would result in about a 20-fold expansion in extracellular volume and cause light scattering.

A characterization of functional properties of lens cells (for review see Mathias et al., 1997) has led to classification of the three zones shown in different colors in Fig. 1. The surface cell zone (S) shown in red includes the anterior epithelium, equatorial differentiating cells, and the basal membranes of differentiating fibers (DFs)* in contact with the posterior surface. The conductance of these cell membranes appears to be selective for $K^+$, and the equatorial cells of this domain provide the majority of lens Na/K ATPase activity (Gao et al., 2000). These cells contribute 2–3% of the total membrane area in a small mouse lens, yet they provide nearly 100% of the $K^+$ conductance and Na/K ATPase activity.

Fiber cells lack Na/K ATPase activity and have relatively low conductance membranes that appear to have lost their $K^+$ channels. The cells have a small $Na^+$ conductance per unit area of membrane, but because of the relatively large area of fiber cell membrane in a lens, the total fiber cell $Na^+$ conductance is significant. Because the fiber cells lack functional Na/K pumps and $K^+$ channels, if they are isolated in physiological saline, they do not maintain a normal negative resting voltage and swell until they burst (Wang et al., 1997). In the lens, we believe fiber cells maintain a negative resting voltage and, thus, constant volume through gap junctional communication with surface cells that have Na/K ATPase activity and $K^+$ channels.

Fiber cell gap junctions contain connexins $\alpha_3$ (Cx46) and $\alpha_8$ (Cx50). The functional and structural properties of these gap junctions change abruptly at the border between differentiating fibers (Fig. 1, DF in blue) and mature fibers (Fig. 1, MF in green). In the peripheral shell of DF, large gap junctional plaques, containing both $\alpha_3$ and $\alpha_8$, occur primarily on the broad sides of equatorial fiber cells (Gong et al., 1998). The coupling conductance is highest in the equatorial region of DF and lowest at either pole (Baldo and Mathias, 1992). Furthermore, DF junctions gate closed in response to acidification (Mathias et al., 1991; Baldo and Mathias, 1992). The sensitivity of DF junctions to pH may not be physiologically relevant, but it demonstrates the capacity for regulation by other physiological signals. In the central core of MF, the structure of gap junctions becomes less well organized, and the junctional plaques are smaller (Kuszak, 1995; Gong et al., 1998). This change in the structure of gap junctional plaques may be due to the cleavage of both $\alpha_3$ and $\alpha_8$ connexin in the DF to MF transition, but not due to synthesis of new proteins since fiber cells lack the machinery necessary for protein synthesis. The coupling conductance of MF is somewhat lower than the average value in DF, it is relatively uniform throughout the core of MF, and it is insensitive to changes in pH (for review see Mathias et al., 1997). This lack of pH sensitivity in MF may have physiological relevance since the intracellular pH there is normally low, owing to lactic acid production by anaerobic metabolism (Bassnett et al., 1987; Mathias et al., 1991).

The most dramatic physiological property of a normal lens is the steady-state current that is illustrated by the lines of flow in Fig. 1. This current is large by epithelial standards, reaching $\sim$30 $\mu A/cm^2$ at either pole or the equator, it is present in lenses from all species studied, and it flows around and through the lens. Thus, one has to believe it is critical for lens homeostasis. Our hypothesis (Mathias et al., 1997) is that this current is coupled to fluid movement, which follows the same pattern and, thus, provides an internal circulatory system for the avascular lens. The localization of membrane transport systems (for reviews see Mathias et al., 1997; Donaldson et al., 2001) suggest the current is carried predominantly by $Na^+$, which flows into the lens along extracellular

*Abbreviations used in this paper:* DF, differentiating fiber; MF, mature fiber.

spaces between cells. Eventually the $Na^+$ is driven by its electrochemical gradient to enter the fiber cells, where it then flows outward from cell to cell via gap junctions, which are concentrated in the equatorial region of DF. Thus, the $Na^+$ flux is directed to equatorial surface cells where Na/K pumps are concentrated to transport it out of the lens, completing the current loops. If fluid follows the same pattern, it would convect glucose along extracellular spaces to inner fiber cells, thus solving one of the lens problems. Indeed, a recent study reports that the glucose facilitator GLUT3 is present in fiber cell membranes (Merriman-Smith et al., 1999). Moreover, Fischbarg et al. (1999) reported fluid movements in the lens. Although our hypothesis on an internal microcirculatory system is not universally accepted, it is consistent with available data. Obviously fiber cell gap junctions are an essential component of the circulation, so knockout of the connexins should affect it. As presented in RESULTS and DISCUSSION, lenses null for either connexin have compromised homeostasis that is consistent with the effect of the knockout on coupling conductance.

Although we have hypotheses on the roles of fiber cell gap junctions in lens physiology, before studies of lenses from the connexin knockout mice, the purpose of the two connexins, $\alpha_3$ and $\alpha_8$, was not known. Both connexins were thought to be present in junctions coupling MF and DF, however, as mentioned above, MF and DF junctions are structurally and functionally different. In our previous study (Gong et al., 1998), we showed that knockout of $\alpha_3$ connexin caused complete uncoupling of MF. Although this demonstrated that $\alpha_3$ connexin is necessary for coupling of MF, it did not rule out the presence of functional $\alpha_8$ connexin in the MF junctions. Moreover, this previous study provided no clues on the purpose of $\alpha_8$ connexin. To better understand the roles of both $\alpha_3$ and $\alpha_8$ connexins in MF and DF junctions, we have produced genetically engineered mice, which lack the gene coding for $\alpha_8$ or $\alpha_3$ connexin. This paper describes the functional properties of gap junctional coupling in lenses lacking $\alpha_8$ connexin and compares these results with those of our previous study (Gong et al., 1998) on lenses lacking the $\alpha_3$ connexin.

## MATERIALS AND METHODS

### *Generation of $\alpha_8$ Connexin Knockout Mice*

The mouse $\alpha_8$ connexin gene was cloned from a 129Sv mouse genomic library by using the mouse $\alpha_8$ connexin gene as a probe (White et al., 1992). The strategy for generating the $\alpha_8$ connexin knockout mice was similar to that described previously for the generation of the $\alpha_3$ connexin knockout mice (Gong et al., 1997). The targeting vector constructs and other experimental details concerning the generation of the $\alpha_8$ connexin knockout mice will be more fully described in a subsequent paper. The $\alpha_8$ connexin mice used in this study were of a mixed background strain (C57 × 129Sv).

### *Immunoblot Analysis of Lens Homogenates*

NaOH-insoluble fractions of lens homogenates from wild-type +/+, heterozygous +/−, and homozygote −/− $\alpha_8$ connexin knockout mice were prepared and analyzed using 10% SDS–polyacrylamide gels, as previously described (Gong et al., 1997). A commercial source of $\alpha_8$ connexin antibody (Alpha Diagnostics) was used at a dilution of 1:500, and a rabbit polyclonal antibody to MIP (1:1,000) and to $\alpha_3$ connexin (1:200) were used for immunoblot analysis (Gong et al., 1997).

### *Electrophysiology*

Because of litter to litter variation in the coupling of wild-type mouse lenses (Gong et al., 1998), comparisons were made between lenses from +/+, $\alpha_8$ +/−, and $\alpha_8$ −/− mice from one litter. In this litter, there were six lenses from each class. Each mouse was killed by intraperitoneal injection of sodium pentobarbitone (57.1 μg per gram body weight), and then its lenses were immediately dissected from the eyes and used for electrophysiological experiments. The dissection and other experimental procedures are identical to those described in Baldo and Mathias (1992) or Mathias et al. (1991). Impedance studies were conducted as follows. One intracellular microelectrode was placed in a fiber cell near the center of the lens, and a small amplitude, wide band current (I) was injected. A second intracellular microelectrode was then placed in a more peripheral fiber cell, and the induced voltage ($\psi_i$) was recorded. The induced voltage and injected current waveforms were sent to a Hewlett Packard Fast Fourier Analyzer, where the frequency domain impedance was computed in real-time. At sinusoidal frequencies above ~100 Hz, the induced voltage response in the intracellular and extracellular compartments within the lens become essentially identical, and $\psi_i \approx IR_S$, where $R_S$ (Ω) is the cumulative series resistance between the point of voltage recording and the lens surface. $R_S$ is proportional to the depth into the lens and the parallel resistivity of the intra- and extracellular compartments; $R_p$ (Ω-cm; Mathias et al., 1991; Gong et al., 1998):

$$R_S = \frac{1}{4\pi}\int_r^a \frac{R_P}{\rho^2}d\rho$$
$$R_P = \frac{R_i R_e}{R_i + R_e}. \quad (1)$$

$R_i$(Ω-cm) is the effective intracellular resistivity, which depends primarily on the gap junctional coupling resistance between fiber cells. $R_e$ (Ω-cm) is the effective extracellular resistivity due to the small tortuous extracellular clefts. In normal physiological conditions, $R_e \gg R_i$, hence $R_p \approx R_i$. In some of the experimental conditions, gap junctional conductance is greatly reduced or zero, in which case $R_p = R_e$. $R_e$ is assumed to be approximately uniform throughout the lens, whereas $R_i$ is lower in DF than MF. The details of the increase in $R_i$ in the DF to MF transition cannot be resolved by our techniques, yet it is clear that the increase occurs over relatively few cell layers. For simplicity, we assume that $R_i$ changes abruptly at the DF to MF transition. Thus, $R_P$ in a well coupled lens is approximately equal to $R_i$, which has the value $R_{DF}$ in the DF zone and $R_{MF}$ in the MF zone. Our initial microelectrode placement recorded $R_S$ in the DF zone and was used to determine $R_{DF}$:

$$R_S \approx \frac{R_{DF}}{4\pi}\left(\frac{1}{r} - \frac{1}{a}\right). \quad (2)$$

The radial location r (measured in centimeters) is the distance of the voltage recording electrode from the lens center, a (measured in centimeters) is the lens radius, and b (measured in centimeters) is the radial location of the transition from DF to MF

(~0.02 cm below the surface). The voltage recording microelectrode was advanced in a series of steps toward the lens center and these recordings were used to determine $R_{MF}$:

$$R_S \approx \frac{R_{DF}}{4\pi}\left(\frac{1}{b}-\frac{1}{a}\right)+\frac{R_{MF}}{4\pi}\left(\frac{1}{r}-\frac{1}{b}\right). \quad (3)$$

To test the sensitivity of coupling to acidification, a measurement of $R_S$ in either DF or MF was made while superfusing the lens with a Tyrode solution that had been bubbled with 100% $CO_2$ (Mathias et al., 1991; Gong et al., 1998). All experiments were performed in normal Tyrode solution at 36–37°C.

## RESULTS

### *Analysis of $\alpha_8$ Knockout Lenses by Immunoblotting*

The $\alpha_8$ connexin gene was disrupted in mice using a strategy that was previously applied for generating the $\alpha_3$ connexin knockout mice (Gong et al., 1997). The successful disruption of the $\alpha_8$ connexin gene was determined by Southern blot and PCR analysis. Connexin expression in lenses from +/+, $\alpha_8$ connexin +/−, and −/− mice was estimated using Western blotting (Fig. 2). Approximately the same amount of material was loaded into each lane, and the intensities of the bands were estimated using a densitometer. This analysis confirmed that the $\alpha_8$ connexin protein was not present in the homozygous $\alpha_8$ −/− mice lenses. Within the accuracy of this technique, in the lenses of heterozygous $\alpha_8$ +/− mice the amount of $\alpha_8$ protein was reduced by ~50% (White et al., 1998). Moreover, the amount of two other lens membrane proteins, $\alpha_3$ connexin and MIP, appeared to be about the same in lenses of wild-type and $\alpha_8$ +/− or −/− mice. The multiple bands present in the $\alpha_3$ blot most likely represent different phosphorylated forms of this connexin.

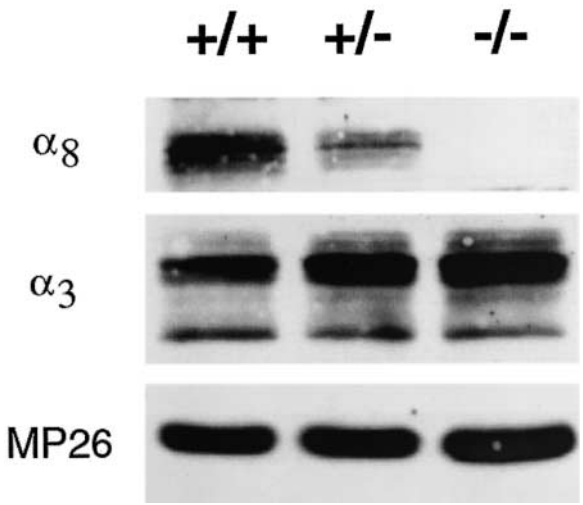


FIGURE 2. Immunoblot of the $\alpha_8$ connexin knockout mice. The NaOH-insoluble protein fractions were prepared from the lenses of +/+, $\alpha_8$ +/−, and $\alpha_8$ −/− mice at the age of 8 wk (Gong et al., 1997). Immunoblot analysis was performed using antibodies against $\alpha_8$ connexin (top), $\alpha_3$ connexin (middle), and MP26 (bottom), respectively. Equal portions of the samples (~15 mg total proteins) were loaded in each lane.

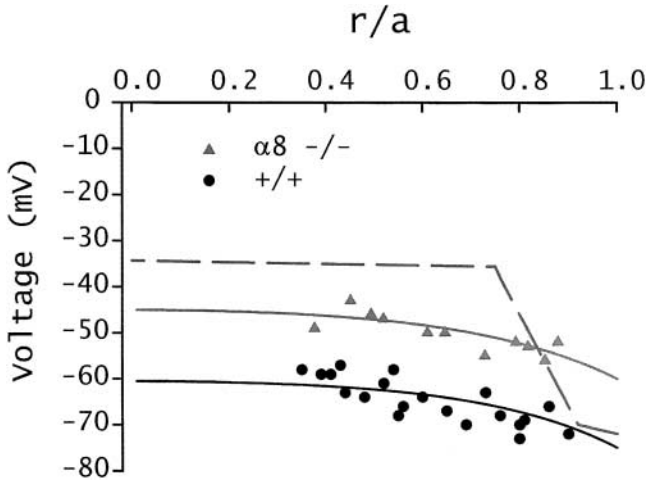


FIGURE 3. Resting voltages. The value of the resting voltage is plotted as a function of normalized distance from the lens center (r/a), where r (in centimeters) is the distance from the center and a (in centimeters) is the lens radius. The points represent data from lenses of +/+ and $\alpha_8$ −/− mice. The solid smooth curves represent the expected distribution of resting voltages based on a model of the circulating current that flows into the lens along extracellular spaces, crosses the fiber cell membrane, and then flows toward the surface of the lens from cell to cell via gap junctions (for review see Mathias et al., 1997). The dashed line is an arbitrary fit to resting voltage data from lenses of $\alpha_3$ −/− mice (Gong et al., 1998). The $\alpha_8$ −/− lenses are depolarized at all locations, suggesting some indirect effects on surface cell membrane permeability. In contrast, the $\alpha_3$ −/− lenses have a normal voltage in DF, but the MF depolarize in a way that reflects loss of gap junctional coupling.

### *Physiological Properties*

As shown by the solid circles in Fig. 3, when the intracellular voltage (measured with respect to the external bathing solution) in a normal mouse lens is graphed as a function of distance from the lens center, there is a voltage gradient with the most central cells having a resting voltage that is 10–15 mV more positive than the peripheral cells (for review see Mathias et al., 1997). This voltage gradient is thought to be associated with the circulating current that flows intracellularly from cell to cell via gap junctions from the center to the surface of the lens. Indeed, the solid line fit to the data is generated from a model of the circulating current (Mathias et al., 1997), however, this model contains several parameters that have not been measured in mouse lenses, so the fit does not provide quantitative information. Nevertheless, it suggests that the mouse lens, like lenses from other species, generates a circulating current. The intracellular voltage in lenses from $\alpha_8$ −/− mice (Fig. 3, triangles) is uniformly depolarized relative to that of wild-type lenses. The input conductance per unit area of lens surface was higher in lenses from

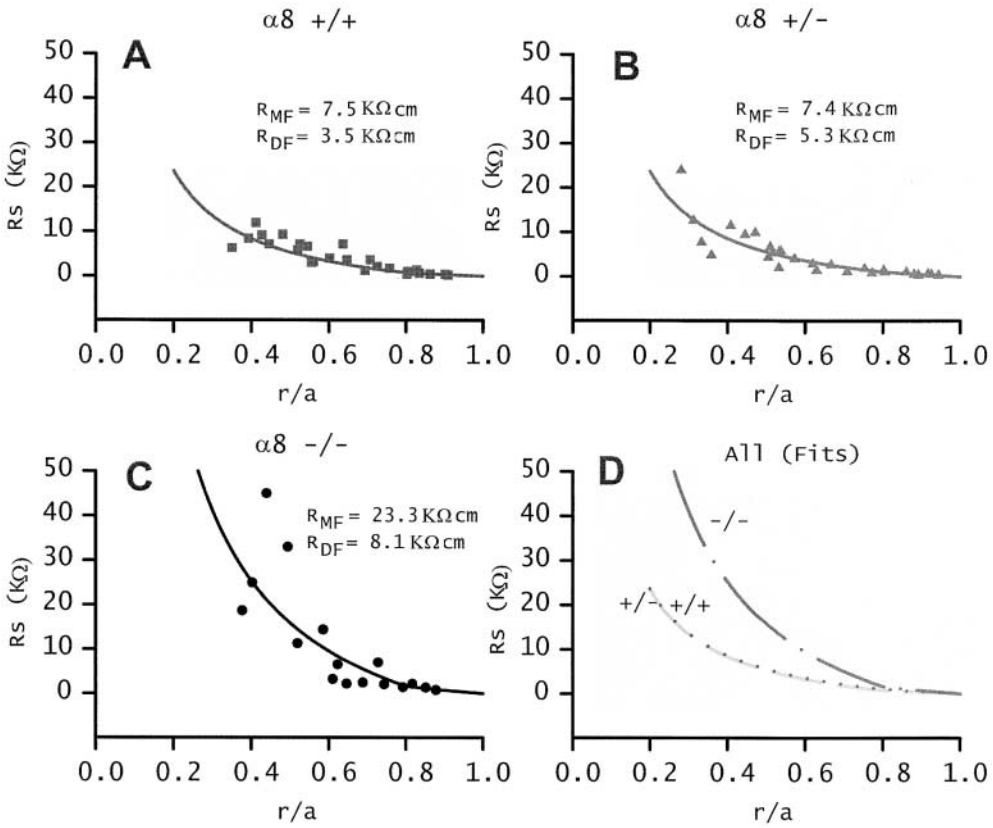


FIGURE 4. The cumulative series resistance ($R_S$). The closed circles in A–C are $R_s$ data from six lenses from +/+, +/−, and −/− $\alpha_8$ connexin knockout mice. The solid lines represent the best fit using Eqs. 2 and 3 with a = 0.101 cm for +/+ and +/− lenses, a = 0.08 cm for −/− lenses, b = 0.8a, and with the values of $R_{DF}$ and $R_{MF}$ listed in each panel. The best fits are graphed together in D. The lenses from $\alpha_8$ −/− mice have many abnormalities that are secondary consequences of the knockout of $\alpha_8$ connexin. The lenses from $\alpha_8$ +/− mice are normal except for changes in coupling conductance. In these lenses, removal of ~50% of $\alpha_8$ connexin significantly increases $R_{DF}$, but has no effect on $R_{MF}$, suggesting the $\alpha_8$ connexin may not be a functional component of gap junctions coupling MF.

−/− mice, with −/− $G_{IN}$ = 1.7 ± 0.3 mS/cm² versus +/+ $G_{IN}$ = 1.4 ± 0.2 mS/cm². The higher conductance and depolarized resting voltage in the $\alpha_8$ connexin knockout lenses indicate effects on transmembrane ion fluxes as well as on cell–cell communication. As initially described in White et al. (1998), the lenses and eyes of $\alpha_8$ −/− mice are abnormally small; for the lenses used in this study, the +/+ radius, a = 0.101 ± 0.001 cm versus the −/− radius, a = 0.080 ± 0.002 cm (mean ± SD, $n$ = 6 each). White et al. (1998) suggested the small lenses and eyes of $\alpha_8$ connexin knockout mice were due to effects during early development. Lenses from −/− $\alpha_8$ mice have reduced transparency (White et al., 1998). Moreover, they are obviously not healthy and tend to run down (input resistance and resting voltage) much more quickly during the course of an experiment than a wild-type lens.

The regional distribution of resting voltage in the $\alpha_3$ versus $\alpha_8$ connexin knockout mice is quite different. The dashed curve in Fig. 3 was generated using resting voltage data from lenses lacking the $\alpha_3$ connexin (Gong et al., 1997). The −/− $\alpha_3$ lenses have a normal voltage and perfectly transparent DF, but they rapidly depolarize in the transition to MF, where there is complete loss of gap junctional coupling. Hence, this distribution of resting voltage may be directly related to the loss of coupling of MF with the surface cells, which possess the lens $K^+$ channels. However, these lenses have a dense central cataract that fills about half the volume of the MF.

Because of the general deterioration of the lenses from either $\alpha_3$ or $\alpha_8$ connexin knockout mice, it is difficult to separate direct from indirect consequences of the lack of a particular connexin. However, lenses from $\alpha_8$ +/− mice were normal with regard to resting voltage, and had the same input conductance as wild-type lenses (+/− $G_{IN}$ = 1.4 ± 0.2 mS/cm²). Similarly, the $\alpha_3$ +/− lenses appeared nearly normal. Thus, reductions in gap junctional conductance in either $\alpha_3$ or $\alpha_8$ connexin +/− lenses are more likely to reflect directly the reduction in the amount of connexin, rather than some secondary effect.

### *The Distribution of Functional $\alpha_3$ and $\alpha_8$ Connexins*

Impedance measurements were conducted on lenses from wild-type and $\alpha_8$ knockout mice and used to generate the data in Fig. 4. These data represent the cumulative series resistance ($R_S$ in Eq. 2 or 3) due to gap junctions coupling fiber cells between the point of recording (r centimeters from the lens center) and the surface of the lens with radius = a cm. Because of spherical geometry, the cumulative resistance increases more than linearly, and because the gap junctional coupling resistance increases in the DF to MF transition, the slope of $R_S$ increases at this transition. As a result of

TABLE I

*Regional Values of Normalized Coupling Conductance*

| | | +/+ | +/− | −/− |
|---|---|---|---|---|
| $\alpha_3$ KO | DF $G_i$ | 1.00 | 0.66 | 0.32 |
| | MF $G_i$ | 0.39 | 0.20 | 0.00 |
| $\alpha_8$ KO | DF $G_i$ | 1.00 | 0.72 | 0.44 |
| | MF $G_i$ | 0.40 | 0.41 | 0.13 |

these two factors, the value of $R_S$ in the MF is almost entirely due to the value of cell–cell coupling resistance of the MF (e.g., see Eq. 4, which separates the contributions of DF and MF to $R_S$). The solid lines represent a best fit to the data using Eqs. 2 and 3, which assume two values of the effective intracellular resistivity ($R_i$): $R_{DF}$ is the value of $R_i$ in DF and $R_{MF}$ is the value in MF (Mathias et al., 1991; Gong et al., 1998). Fig. 4 D shows an overplot of the fits to the data from $\alpha_8$ connexin +/+, +/−, and −/− mice. $R_{DF}$ is accurately determined from the first (outermost) measurement of $R_S$. Note that the fits to +/+ and +/− data virtually overlay even though $R_{DF}$ is significantly higher in the +/− data (see Table I). This is because $R_{MF}$ is about the same in these two classes of lenses, and as noted above, $R_{MF}$ dominates the value of $R_S$ as one records near the center of the lenses. If the effective intracellular resistivity is multiplied by the fiber cell width, $w \approx 3$ μm, the reciprocal of that product is approximately the gap junctional coupling conductance per area of cell–cell contact. For example, in lenses from +/+ mice, $R_{DF} = 3.5$ KΩ-cm and $1/(R_{DF}\, w) = 1.05$ S/cm$^2$.

Table I summarizes the normalized coupling conductance based on the values of $R_{DF}$ and $R_{MF}$ in Fig. 4, and on the average conductances from the $\alpha_3$ knockout mice studied in Gong et al. (1998). To facilitate comparison, the values are normalized to the coupling conductance of DF in the +/+ mouse lenses. However, as calculated above, that conductance is very close 1 S/cm$^2$, so Table I can be interpreted approximately as the coupling conductance per area of cell–cell contact.

In lenses +/− for either $\alpha_3$ or $\alpha_8$ connexin, there is about a 30% reduction in the coupling conductance of DF, and in lenses from the −/− mice the coupling conductance is reduced by 60–70%. If each connexin contributed equally to the coupling conductance of DF, lenses from mice +/− for either connexin should have a 25% reduction in coupling conductance, and lenses from −/− mice should have a 50% reduction. However, in Table I the reductions are greater, as if each connexin contributed more than half the conductance. One should keep in mind that these numbers were derived from fitting the data in Fig. 4. When generating data like those in Fig. 4, it is difficult to accurately locate the position of the tip of the voltage recording microelectrode relative to spherical coordinates within the lens. This is a major source of scatter, which leads to uncertainty in the derived values of coupling conductance. Moreover, as just described, the lenses from −/− mice were obviously abnormal and there are likely to be indirect effects related to their poor health. With these limitations in mind, our interpretation of the data in Table I is that both connexins are functionally important in the DF and each connexin contributes about equally to the coupling conductance of DF.

Comparison of the conductances in the MF of the heterozygous lenses indicates that $\alpha_3$ +/− lenses have reduced coupling, whereas $\alpha_8$ +/− lenses have the same conductance as wild type. This suggests $\alpha_8$ connexin may not have a functional role in the coupling of MF. In lenses from $\alpha_3$ connexin −/− mice, the coupling conductance of MF is zero, which is also consistent with lack of functional $\alpha_8$ connexin in this domain. As described earlier, indirect effects in the lenses from connexin −/− mice are of concern. However, the abrupt reduction of coupling conductance to zero in the DF to MF transition cannot be simply attributed to an indirect effect. Moreover, because of the way the lens grows, the MF of these lenses were DF a week or two earlier, and at that stage, they were well coupled by junctions made of $\alpha_8$ connexin. Note that DF of lenses from $\alpha_3$ connexin −/− mice are well coupled by the standards of most cells, though the conductance is somewhat reduced from normal. Consideration of all these factors suggests that $\alpha_8$ connexin is not functional in the MF. However, inconsistent with this hypothesis, lenses from $\alpha_8$ −/− mice show a reduction in MF coupling conductance. Nevertheless, these lenses are grossly abnormal and there are several indirect effects, such as reduced lens size, increased input conductance, and depolarized resting voltage. Therefore, the reduced coupling may be an indirect effect of the $\alpha_8$ knockout. For example, intracellular $Ca^{2+}$ homeostasis may be compromised, there may be abnormal protease activity, etc., leading to reductions in coupling conductance. The simplest interpretation of the changes in MF conductance is that the DF to MF transition results in a loss of functional $\alpha_8$ connexin, which in turn reduces the coupling conductance and leaves $\alpha_3$ as the only functional connexin.

### *Gap Junctional Gating*

Cytoplasmic acidification has been shown to gate gap junctions closed in the DF region, but not in the MF region, of normal lenses from frog (Mathias et al., 1991), rat (Baldo and Mathias, 1992), and mouse (Fig. 5). It has been assumed that this reflects the presence of intact connexin in the junctions coupling the DF, as well as the capacity for physiological regulation, whereas cleavage of the connexins that occurs in the transition from DF to MF results in the loss of this capacity. Fig. 5

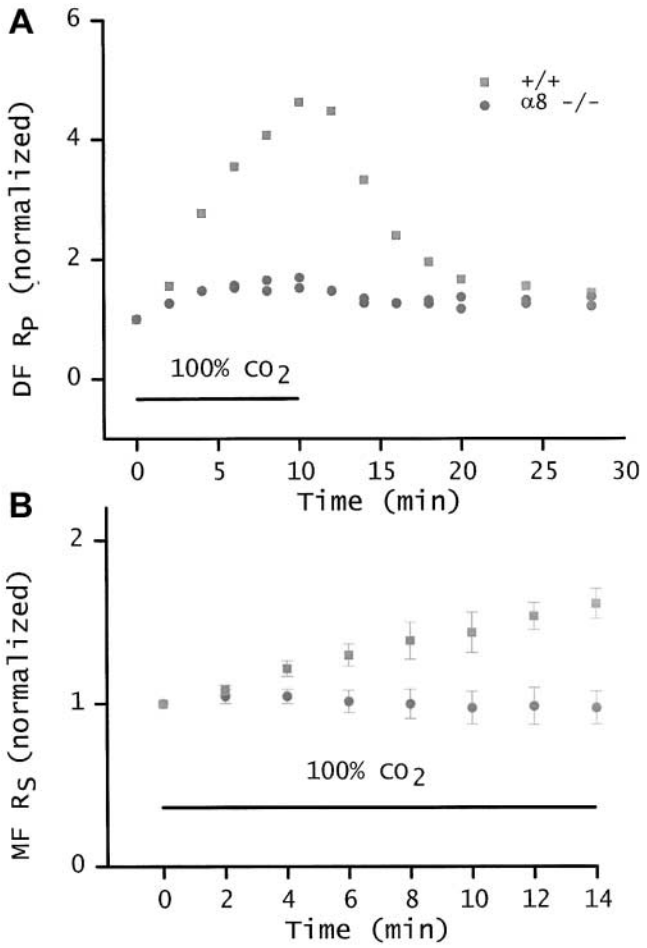


Figure 5. pH-sensitive gating. A compares the coupling of DF from wild-type and $\alpha_8$ connexin −/− lenses when superfused with Tyrode bubbled with 100% $CO_2$. The $CO_2$-saturated solution was superfused during the time period indicated by the bar. The initial values of $R_P$. $R_{DF}$ for the two −/− lenses was 5.9 and 10.1 KΩ-cm, whereas the initial value of $R_P$ in the +/+ lens was 3.4 KΩ-cm, and all of these values were stable before $CO_2$ exposure. To facilitate comparison, each resistivity was normalized to its initial value, and then graphed as a function of time. In a 10-min exposure to 100% $CO_2$, the $R_P$ of DF in the wild-type lens increased 4.7-fold. This was a typical response, similar to the responses we recorded from a number of lenses from wild-type mice of different litters. In contrast, $R_P$ of the DF in $\alpha_8$ −/− lenses increased only 1.6-fold. Thus, in the $\alpha_8$ −/− lens, homotypic channels made from $\alpha_3$ connexin have little or no sensitivity to pH. The surface cells express $\alpha_1$ (Cx43) connexin, so the limited pH gating seen in A could be due to $\alpha_1$. B compares the cumulative series resistance ($R_S$ in Eq. 3) in lenses from +/+ and $\alpha_8$ −/− mice. Again, the $CO_2$ exposure was during the period indicated by the bar and before t = 0, the values of $R_S$ were stable. As illustrated by Eq. 4, this resistance is dominated by the contribution of MF. Again, the resistances were normalized to their initial values, and then graphed as a function of time exposed to 100% $CO_2$. The +/+ data were mean ± SD from four lenses. Although the MFs of +/+ lenses are not sensitive to pH, DFs are sensitive, hence, $R_S$ increases significantly. The $\alpha_8$ −/− data are mean ± SD from three lenses. In the $\alpha_8$ −/− lenses, all fiber cell gap junctions contain homotypic channels made up of $\alpha_3$ connexin. If the small increase in resistance of DF from $\alpha_8$ −/− mice shown in A is confined to DF or surface cells, it will be a very small fraction of the total $R_S$ shown in B. Indeed, the total $R_S$ of $\alpha_8$ −/− mice shows no significant increase on exposure of the lenses to 100% $CO_2$.

A shows that the ability of junctions between DF to gate closed depends on the presence of $\alpha_8$ connexin.

We have determined the sensitivity of the gap junctions to cytoplasmic acidification in the DF and MF of $\alpha_8$ knockout lenses (Fig. 5). Fig. 5 A compares the effect of 100% $CO_2$ on DF junctional resistance in +/+ and −/− $\alpha_8$ lenses. To facilitate this comparison, resistances are normalized to their initial values. In a 10-min exposure to 100% $CO_2$, $R_P$ (Eqs. 1 and 2) in lenses lacking $\alpha_8$ connexin increased by a factor of only 1.6, whereas $R_P$ in wild-type DF increased 4.7-fold. This suggests that homotypic $\alpha_3$ channels in the lens have a very limited ability to gate in response to acidification and that regulation of DF coupling requires the presence of $\alpha_8$ connexin. Indeed, the 1.6-fold increase in series resistance is very rapid and could be due to effects only on surface cell junctions, where $\alpha_1$ (Cx43) is the dominant connexin.

Fig. 5 B shows the effect of 100% $CO_2$ on the total coupling resistance of DF in series with a significant fraction of MF. Owing to spherical divergence of current flow, the resistance of the MF dominates, and the closure of channels in DF has a relatively smaller effect than that shown in Fig. 5 A. Based on Eq. 3 and a typical measurement where the +/+ lens radius a = 0.101 cm, the DF extends from radial location b to a, b = 0.8a, and the resistance is measured r centimeters from the lens center, r = 0.4a:

$$R_S \cong \underset{\text{DF}}{690\Omega} + \underset{\text{MF}}{9,000\Omega}. \tag{4}$$

The resistance values in Eq. 4 represent typical +/+ contributions of DF and MF to $R_s$. Our interpretation of the data from +/+ lenses is that $CO_2$ has no effect on $R_{MF}$, but causes the resistance of +/+ DF to go from ~690 to ~6,900 Ω (i.e., $R_P$ varies from 3.5 to 35 KΩ-cm). Thus, the effect on total $R_s$ is measurable but fractionally much smaller than that shown in Fig. 5 A. In the lenses lacking $\alpha_8$ connexin, the resistance of DF increases by a factor of 1.6, according to Fig. 5 A. This would represent about a 4% increase in total $R_s$ of $\alpha_8$ −/− lenses (Fig. 4) and would not be easily detectable, assuming $R_{MF}$ is not sensitive to $CO_2$. Indeed, Fig. 5 B shows no detectable increase in $R_s$ for the $\alpha_8$ −/− lenses, providing direct evidence that homotypic $\alpha_3$ channels in MF are unable to gate in response to changes in pH, just as has been observed in other lenses (for review see Mathias et al., 1997). Moreover, these data confirm the lack of pH-sensitive gating of DF junctions in lenses from $\alpha_8$ connexin −/− mice.

In 10 min, the effect of $CO_2$ on the $\alpha_8$ −/− lenses is essentially complete, whereas homotypic $\alpha_8$ channels (in $\alpha_3$ −/− lenses; Gong et al., 1998) or wild-type mixed $\alpha_3$ and $\alpha_8$ channels continue to close for ~30 min. Typical final values (after 30 min) of $R_P$ in two lenses from +/+ mice were 38 and 45 KΩ-cm. Curve

fits of full impedance datasets (0.01–1,000 Hz) from lenses in normal Tyrode (no bubbling with $CO_2$) of +/+ mice gave an average value of $R_e$ of 27 ± 17 KΩ-cm (mean ± SD, $n = 11$). If $R_e$ were the same after bubbling with 100% $CO_2$, the value of $R_P$ should not have exceeded 27 KΩ-cm (i.e., $R_i \rightarrow \infty$ in Eq. 1, yields $R_P = R_e$). In 2 of the 11 fits, the values of $R_e$ exceeded 40 KΩ-cm, so it is possible that the $CO_2$ data were from lenses with unusually high values of $R_e$. However when lenses are exposed to $CO_2$, their resting voltage depolarizes significantly (Mathias et al., 1991; Baldo and Mathias, 1992); the above 2 mouse lenses had final resting voltages of −28 and −26 mV. Depolarization normally leads to cell swelling and a very small increase in intracellular volume would lead to a significant decrease in extracellular volume within the lenses and thus increase $R_e$. The final recorded values of $R_P$ therefore suggest total closure of all DF junctions and possibly some collapse of the extracellular spaces causing an increase in $R_e$. In 2 lenses from $\alpha_3$ −/− mice, the final values of $R_P$ were even larger (92 and 89 KΩ-cm). In these lenses, we were unable to obtain reasonable curve fits to impedance data using our equivalent circuit model of a normal lens, so the value of $R_e$ is not known. Thus, we cannot know for certain if the larger final values of $R_P$ have any significance with regard to closure of gap junction channels. Nevertheless we think it is unlikely, since any time the value of $R_P$ exceeds ~27 KΩ-cm, all gap junction channels have probably closed. Thus we interpret these data as the total closure of all the homotypic $\alpha_8$ channels in DF junctions.

The data in Fig. 5 suggest homotypic $\alpha_3$ channels are not closed by a drop in pH. If +/+ DF junctions comprise homotypic, independent $\alpha_3$ and $\alpha_8$ channels, which are parallel resistance paths, then the final resistance (following exposure to 100% $CO_2$) between DF of +/+ lenses should not be greater than that recorded in the $\alpha_8$ −/− lenses, which have homotypic $\alpha_3$ channels. However, the final resistivity in lenses lacking the $\alpha_8$ connexin was 9–18 KΩ-cm, whereas that of +/+ lenses was 38–45 KΩ-cm. Thus the presence of $\alpha_8$ connexin enables the total closure of all gap junction channels in DF of +/+ mice. These data suggest synergy between the $\alpha_3$ and $\alpha_8$ connexins, inasmuch as channels in junctional plaques containing mixed connexins gate closed more efficiently than would be expected for homotypic, independent channels. The simplest explanation for this observation is that all DF channels are heteromers, containing a mix of $\alpha_3$ and $\alpha_8$ subunits, with one $\alpha_8$ subunit being sufficient to cause closure of each channel. However, one must also consider indirect effects of loss of $\alpha_8$ connexin, such as changes in posttranslational processing of $\alpha_3$ connexin. Whatever the mechanism, this was an unexpected and unique observation that one connexin is regulated by the presence of another.

## DISCUSSION

The data presented here in connection with previous results (Gong et al., 1998) suggest the $\alpha_3$ and $\alpha_8$ connexins have distinct roles in lens gap junctional communication: $\alpha_3$ connexin is necessary for the coupling of MF, whereas $\alpha_8$ connexin is necessary for the pH-sensitive gating of junctions coupling DF.

MF in lenses from mice lacking the $\alpha_3$ connexin also lack coupling. Lenses from $\alpha_3$ +/− mice have ~50% less $\alpha_3$ connexin than wild-type lenses (based on quantitative Western blotting), and their MF have ~50% less coupling conductance. Similarly, lenses from $\alpha_8$ +/− mice have ~50% less $\alpha_8$ connexin than wild type, but in contrast, their MF have the same coupling conductance as wild-type lenses. These data suggest MF coupling conductance depends directly on the amount of $\alpha_3$ connexin and is independent of the amount of $\alpha_8$ connexin. This suggests that MF junctions do not contain functional $\alpha_8$ connexin. The one observation inconsistent with this hypothesis is the drop in MF coupling conductance in the lenses from $\alpha_8$ −/− mice. Many physiological properties of these lenses were abnormal, however, and it would be surprising if there were not some indirect effects on gap junctional conductance. Perhaps the more telling observation is that the MF are still well coupled in the $\alpha_8$ connexin knockout lenses.

Both connexins contribute about equally to the coupling conductance of DF. However, in the absence of $\alpha_8$ connexin, the lens homotypic $\alpha_3$ channels are unable to respond to a change in pH, whereas in the presence of $\alpha_8$ connexin, all DF junctional channels gate closed in response to acidification. Thus, the presence of $\alpha_8$ connexin may regulate the conductance contributed by $\alpha_3$ connexin.

The simplest explanation for the synergistic gating between the $\alpha_3$ and $\alpha_8$ connexins would be heteromeric channels (Jiang and Goodenough, 1996). For example, if all gap junctional channels of DF were made from a mix of $\alpha_3$ and $\alpha_8$ connexins and if only one $\alpha_8$ subunit were sufficient to cause closure, then the gating data presented here would be explained. However, the simplest model to explain the MF conductance changes shown in Table I is that MF communication is via homotypic $\alpha_3$ channels. But if the channels are homomers in the MF, one would expect that they started out as homomers in the DF, which is inconsistent with the simplest explanation of DF gating. Therefore, a more complex model is necessary to explain both observations. A number of increasingly complex hypotheses can be formulated, but the available data do not distinguish the possibilities. Higher resolution biochemical and biophysical characterization of channels in both DF and MF is needed to provide a basis for a hypothesis on molecular mechanism.

In all species studied, the DF to MF transition results in a loss of gap junctional gating in response to acidification (for review see Mathias et al., 1997). The DF to MF transition also results in cleavage of each connexin's COOH terminus, which was shown to be the pH-sensitive gate for the $\alpha_8$ connexin (Lin et al., 1998). The data presented here suggest that, in the lens, the $\alpha_3$ connexin is not pH sensitive, even in DF where this connexin is thought to be intact, at least in wild-type lenses. Thus, regardless of the connexin structure or composition of lens gap junction channels, these data imply coupling of MF would be insensitive to pH. Therefore, the more perplexing issue is the mechanism of pH gating of DF junctions. Interestingly, when exogenously expressed in oocytes, homotypic $\alpha_3$ junctions are sensitive to pH (White et al., 1994), unlike the lens homotypic $\alpha_3$ junctions in the DF of $\alpha_8$ knockout mice. This difference in the properties of endogenous and exogenously expressed $\alpha_3$ connexin may reflect the presence of different regulatory proteins, or it may be due to differences in posttranslational processing. Understanding this difference may lead to a better understanding of gap junctional gating in DF of the lens.

In the INTRODUCTION, we suggested two major roles for lens gap junctions: (1) setting the resting voltage of inner fiber cells and, thus, maintaining volume regulation in these cells; and (2) conducting the lens circulation to the inner fiber cells and, thus, providing delivery of glucose for metabolism and homeostasis. In lenses from $\alpha_3$ $-/-$ mice, MF were uncoupled from the surface cells. These fibers had a depolarized resting voltage that is consistent with hypothesis 1. Moreover, the central MF had a complete breakdown in homeostasis and developed a dense cataract that is consistent with hypothesis 2. These observations, of course, do not prove the hypotheses, but once again the data fail to contradict them. Surprisingly, it appears that these roles depend on the presence of $\alpha_3$ connexin and are lost when $\alpha_8$ is the only fiber cell connexin. Thus, the expression of $\alpha_3$ connexin in fiber cells is apparently the lens resolution to the problem of maintaining gap junctional communication throughout the life of fiber cells where connexin turnover is not possible. Lenses from $\alpha_8$ $-/-$ mice had reduced gap junctional coupling, but MF remained in communication with the surface cells. Although these lenses were clearly compromised, they did not develop a dense central cataract, which is consistent with the presence of a reduced circulation. The major difference between coupling of fiber cells in $+/+$ versus $-/-$ $\alpha_8$ knockout lenses was the loss of pH sensitivity in DF junctions. Yet, the $\alpha_8$ $-/-$ lenses display many secondary changes, such as reduced size, altered membrane transport, depolarized resting voltage, and rapid deterioration after dissection. It is possible that all of these secondary effects are a consequence of loss of gating. The lack of $\alpha_8$ connexin is thought to disrupt early development (White et al., 1998). Perhaps there is a stage in early development when gap junctional communication needs to be shut down for normal cell division and protein expression to occur. Again, this is an intriguing possibility, and one that needs further investigation. Therefore, it appears that each question answered by these studies has raised even newer questions, the exploration of which is central to our understanding of the lens.

We would like to dedicate this paper to Dr. Bernie Gilula, who passed away on September 27, 2000. To those of us at Scripps, Bernie was a mentor, close colleague, and friend. To those of us at SUNY, he was a valued collaborator and friend. We shall all miss him.

This work was supported by the National Institutes of Health grants EY06391 (to R.T. Mathias), EY11093 (to N.M. Kumar), EY12142 (to N.B. Gilula and N.M. Kumar) and GM37904 (to N.B. Gilula).

*Submitted: 9 July 2001*
*Revised: 17 September 2001*
*Accepted: 18 September 2001*

REFERENCES

Baldo, G.J., and R.T. Mathias. 1992. Spatial variations in membrane properties in the intact rat lens. *Biophys. J.* 63:518–529.

Bassnett, S., P.C. Croghan, and G. Duncan. 1987. Diffusion of lactate and its role in determining intracellular pH in the lens of the eye. *Exp. Eye Res.* 44:143–147.

Donaldson, P., J. Kistler, and R.T. Mathias. 2001. Molecular solutions to lens transparency. *News Physiol. Sci.* 16:118–123.

Fischbarg, J., F.P. Diecke, K. Kuang, B. Yu, F. Kang, P. Iserovich, Y. Li, H. Rosskothen, and J.P. Koniarek. 1999. Transport of fluid by lens epithelium. *Am. J. Physiol.* 276:C548–C557.

Gao, J., X. Sun, V. Yatsula, R.S. Wymore, and R.T. Mathias. 2000. Isoform-specific function and distribution of Na/K pumps in the frog lens epithelium. *J. Membr. Biol.* 178:89–101.

Gong, X., E. Li, G. Klier, Q. Huang, Y. Wu, H. Lei, N.M. Kumar, J. Horwitz, and N.B. Gilula. 1997. Disruption of alpha3 connexin gene leads to proteolysis and cataractogenesis in mice. *Cell.* 91: 833–843.

Gong, X., G.J. Baldo, N.M. Kumar, N.B. Gilula, and R.T. Mathias. 1998. Gap junctional coupling in lenses lacking alpha3 connexin. *Proc. Natl. Acad. Sci. USA.* 95:15303–15308.

Jiang, J.X., and D.A. Goodenough. 1996. Heteromeric connexons in lens gap junction channels. *Proc. Natl. Acad. Sci. USA.* 93:1287–1291.

Kuszak, J.R. 1995. The ultrastructure of epithelial and fiber cells in the crystalline lens. *Int. Rev. Cytol.* 163:305–350.

Lin, J.S., R. Eckert, J. Kistler, and P. Donaldson. 1998. Spatial differences in gap junction gating in the lens are a consequence of connexin cleavage. *Eur. J. Cell Biol.* 76:246–250.

Mathias, R.T., J.L. Rae, and G.J. Baldo. 1997. Physiological properties of the normal lens. *Physiol. Rev.* 77:21–50.

Mathias, R.T., G. Riquelme, and J.L. Rae. 1991. Cell to cell communication and pH in the frog lens. *J. Gen. Physiol.* 98:1085–1103.

Merriman-Smith, R., P. Donaldson, and J. Kistler. 1999. Differential expression of facilitative glucose transporters GLUT1 and GLUT3 in the lens. *Invest. Ophthalmol. Vis. Sci.* 40:3224–3230.

Wang, L.F., P. Dhir, A. Bhatnager, and S.K. Srivastava. 1997. Contribution of osmotic changes to disintegrative globulization of sin-

gle cortical fibers isolated from rat lens. *Exp. Eye Res.* 65:267–275.
White, T.W., R. Bruzzone, D.A. Goodenough, and D.L. Paul. 1992. Mouse Cx50, a functional member of the connexin family of gap junction proteins, is the lens fiber protein MP70. *Mol. Biol. Cell.* 3:711–720.
White, T.W., R. Bruzzone, S. Wolfram, D.L. Paul, and D.A. Goodenough. 1994. Selective interactions among the multiple connexin proteins expressed in the vertebrate lens: the second extracellular domain is a determinant of compatibility between connexins. *J. Cell Biol.* 125:879–892.
White, T.W., D.A. Goodenough, and D.L. Paul. 1998. Targeted ablation of connexin50 in mice results in microphthalmia and zonular pulverulent cataracts. *J. Cell Biol.* 143:815–825.